Quaternary International 507 (2019) 206–216

Contents lists available at ScienceDirect

Quaternary International

journal homepage: www.elsevier.com/locate/quaint

Resonance of the '4.2ka event' and terminations of global civilizations during the Holocene, in the palaeoclimate records around PT Tso Lake, Eastern Himalaya

Nivedita Mehrotra[a], Santosh K. Shah[a,*], Nathani Basavaiah[b], Amzad H. Laskar[c], Madhusudan G. Yadava[d]

[a] Birbal Sahni Institute of Palaeosciences, 53–University Road, Lucknow, 226 007, India
[b] Indian Institute of Geomagnetism, Navi Mumbai, Maharashtra, India
[c] National Sun Yat-Sen University, Department of Chemistry, 70 Lin-Hai, Kaohsiung, 80424, Taiwan
[d] Physical Research Laboratory, Ahmedabad, Gujrat, India

ARTICLE INFO

Keywords:
4.2ka event
Bronze age civilizations
Multi–proxy data
Temperature reconstruction
PT Tso lake
Eastern Himalaya

ABSTRACT

Climate driven changes have impacted various civilizations and have major influence on human population globally. Remote regions such as the Himalaya also archived these climatic events in various proxies. The Eastern Himalaya region has recorded the Holocene climate change events in numerous proxy records. A multi–proxy record of the early to late–mid Holocene climate change from the catchment of PankangTeng Tso (PT Tso) Lake at an altitude of 3935 m asl in the Tawang district of Arunachal Pradesh was studied. A 90 cm sediment profile showed a synchronous pattern of Holocene climate changes in the palynological, environmental magnetic and carbon isotope data recorded. Dominant cold-humid conditions at 4625 cal yr BP followed by a cold-dry period was documented in the proxy data. The vegetation vis–à–vis climate varied throughout the Holocene and cold–dry conditions along with sub-alpine vegetation prevailed in the region around the "4.2ka event". Human activities and environmental changes in the Tawang district during the Holocene probably impacted the vegetation during this significant period of the development and demise of major global civilizations.

1. Introduction

The abrupt climate change (ACC) during the Early to Middle Holocene around 4000 cal yr BP was observed in many proxy records from western Asia (Cullen et al., 2000), eastern Asia (Liu and Feng, 2012), Europe (Drysdale et al., 2006; Roland et al., 2014), North America (Booth et al., 2005), South America (Marchant and Hoogiemstra, 2004), Africa (Thompson et al., 2002) and the North Atlantic (Bond et al., 2001). This "4.2 ka Event", a multi-decadal to multi-centurial drought, possibly led to the collapse of many civilizations and the abandonment of cities in ancient India, ancient Egypt, and Mesopotamia (Singh, 1971; Singh et al., 1990; Weiss et al., 1993; Dalfes et al., 1997; Possehl, 1997; Enzel et al., 1999; Weiss, 2000; deMenocal, 2001; Weiss and Bradley, 2001; Staubwasser et al., 2003; Drysdale et al., 2006; McDonald, 2011; Clift et al., 2012; Dixit et al., 2014; Sarkar et al., 2016). There were drastic changes in the climate and monsoon strength during the ACC events (Hong et al., 2003; McDonald, 2011; Berkelhammer et al., 2012). These were probably caused by variations in solar radiation and abrupt ocean surface cooling in the North Atlantic (Bond et al., 2001; Hong et al., 2003; Staubwasser et al., 2003; Dixit et al., 2014 and references therein).

Here we present a study of a sediment profile collected near the catchment of the PankangTeng Tso (PT Tso) Lake in the Tawang district of Arunachal Pradesh, Eastern Himalaya. The palynological, mineral magnetism and carbon isotope data of this sediment profile recorded simultaneously the Early–Middle Holocene ACC events at the present site.

2. Regional setting

The profile sampling site is located along the slope of the valley surrounding the PT Tso Lake (27°46.85′N and 91°58.38′E; 3935 m asl) which is about 18 km from Tawang township in the Tawang district of Arunachal Pradesh, Eastern Himalaya (Fig. 1 and supplementary material). These Holocene sediments have similar ages as the newer alluvium of the Hapoli formation underlain by the older alluvium in the

* Corresponding author.
E-mail addresses: santoshk.shah@gmail.com, santoshkumar_shah@bsip.res.in (S.K. Shah).

https://doi.org/10.1016/j.quaint.2018.09.027
Received 18 January 2018; Received in revised form 17 May 2018; Accepted 17 September 2018
Available online 19 September 2018
1040-6182/

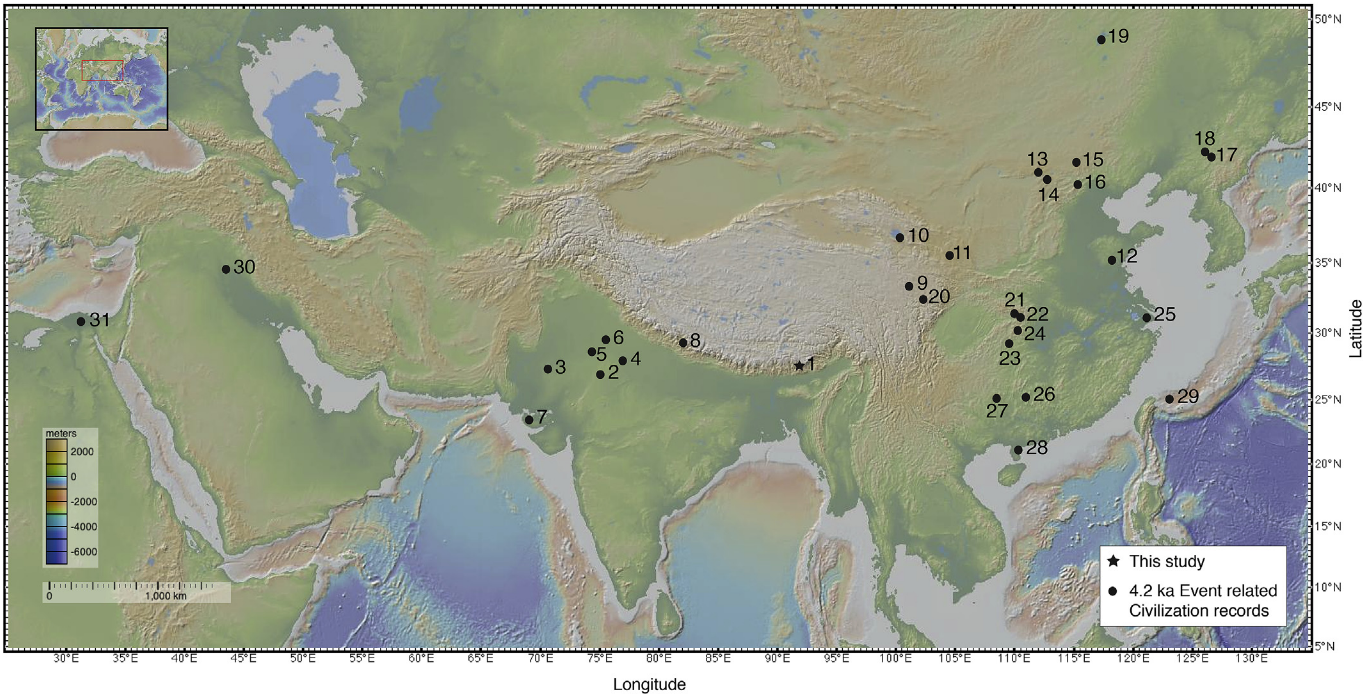

Fig. 1. Locations of present study site and palaeoclimatic records described civilization in relation to 4.2k events. Details of the location are 1 PTTL (Present study site); 2 NW India (Enzel et al., 1999; Prasad and Enzel, 2006; MacDonald, 2011); 3 Harappan sites (Giosen et al., 2012); 4 Kotla Dahar (Dixit et al., 2014); 5 Karsandi palaeolake (Dixit et al., 2018); 6. Bhirrana (Sarkar et al., 2016): 7. Harapan sites (Pokharia et al., 2017); 8 Rara Lake (Nakamura et al., 2016); 9 Ximencuo Lake (Mischke and Zhang, 2010); 10 Qinghai Lake (Shi and Kong, 1992; Shi et al., 1993; Liu et al., 2002); 11 Sujiawan Section (Feng et al., 2004, 2006); 12 Baahar Nuur Lake (Gao et al., 2007); 13 Diajiaohaizi Section (Wang and Wang, 1992; Zhang et al., 1997); 14 Daihai Lake (Liu and Feng, 2012); 15 Bayanchagan Lake (Jiang et al., 2006); 16 Taishizhuang Section (Jin and Liu, 2002; Tarasov et al., 2006); 17 Hani Peat (Hong et al., 2005); 18 Jinchuan Peat (Hong et al., 2001); 19 Hulun Lake (Wen et al., 2010a, 2010b); 20 Hongyuan Peat (Hong et al., 2003); 21 Dajiu Lake (Zhu et al., 2007); 22 Shanbao Cave (Shao et al., 2006); 23 Linhuan Cave (Cosford et al., 2008); 24 Heshang Cave (Hu et al., 2008); 25 Taihu Lake (Chen et al., 2005; Tao et al., 2006); 26 Xiangshui Cave (Zhang et al., 2004); 27 Dongge Cave (Dykoski et al., 2005; Wang et al., 2005); 28 Huangguangyan Maar (Zheng et al., 2003; Wang et al., 2007); 29 Core 255 (Jian et al., 2000); 30 Tell Leilan Syria (Weiss et al., 1993) and 31 Nile Delta, Egypt (Stanley et al., 2003). Note: Location 2, 3, 4 and 6 are many sites. Locations 10 to 29 are described in Liu and Feng (2012).

Quaternary deposits of Arunachal Pradesh (Kesari et al., 2010). These Quaternary alluvial deposits are found along major river valleys in most parts of Arunachal Pradesh and the Eastern Himalayas. These Quaternary sediments are underlain by the Siwalik group of rocks and other formation sequences generally occupying the Himalayan belt in Arunachal Pradesh (Kesari et al., 2010).

The vegetation distribution in Arunachal Pradesh is comprised of tropical, subtropical, temperate (broad leaved and conifers), sub-alpine to alpine forest. Various factors such as the varied topography, phytogeographical location, and a discrete variation in the climate of Arunachal Pradesh (Baishya et al., 2002) contribute to this varied distribution. The various plant species occupy an altitude range of 2438–3658 m asl in the Tawang district. At lower altitudes from along the Tawang Chu river basin and upto 2438 m asl are found the *Pinus wallichiana*, *Alnus*, *Rhododendron, Salix,* etc. which precede the Oak forest that persist up to 3048 m asl. The forests are dominated by Fir, *Tsuga*, *Rhododendron*, *Magnolia*, *Taxus baccata* from 3048 m asl to 3658 m asl. Then up to an altitude of 3962 m asl, the forest are comprised of Fir, *Abies densa*, and *Juniper*. These are followed by short, branchy *Rhododendron,* alpine shrubs along with alpine pasture at higher altitudes (Biswal, 2006).

There are very few long-term instrumental climate records available in the eastern Himalaya region and also in the Tawang district (Bhattacharyya and Chaudhary, 2003). The district-wise rainfall records of Arunachal Pradesh, spanning only five years is given by the Indian Meteorological Department (http://hydro.imd.gov.in/hydrometweb/). Due to the dearth of long-term climate records we interpolated and down-scaled the CRU TS 3.22 gridded climate data for the present study site for 1901–2013 C.E. The interpolation was based on inverse distance weighting over the four nearest grid points covering the area between 27°00′-28°00′ N and 91°30′-92°30′ E closest to our sampling site. According to the Walter and Leith climate diagram (Walter and Leith, 1967) based on the interpolated climate of the study site the minimum mean minimum temperature, maximum mean maximum temperature, mean annual temperature and mean annual precipitation was −5.6 °C, 21.4 °C, 10.4 °C and 683 mm respectively (Fig. 2). The maximum precipitation received at the study site was in the southwest monsoon season, between the months of July–-September.

3. Material and methods

3.1. Lithology and age depth model

A 90 cm long sediment profile collected along the catchment of the PT Tso Lake (henceforth PTTL) had silty clay sediments up to 38 cm which were rich in organic matter. This was followed by a few cm of sandy clay having a few pebbles and again some silty clay with a little sand content. The profile PTTL is mostly comprised of sandy clay mixed with few silty clay layers along with pebbles below 49 cm (see supplementary material).

The sediments at different depths of the profile PTTL was dated at the Physical Research Laboratory, Ahmedabad, India. The ^{14}C dates were calibrated using the clam, ‘classical’ age-depth modeling software (Blaauw, 2010; R statistical software package). For the calibration we used the northern hemisphere terrestrial curve IntCal13.14C from Reimer et al. (2013). The age-depth model was developed using a linear regression model (see supplementary material). The ages of the sediments beyond ^{14}C date of 4600 ± 100 years were extrapolated. Thus, based on the four calibrated ages in calendar years BP (cal yr BP) of the

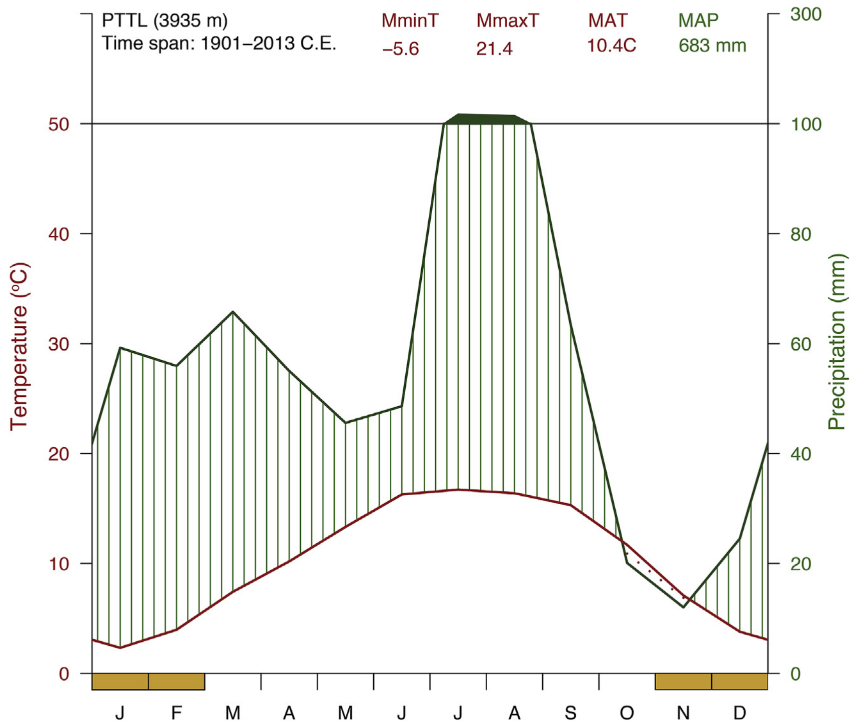

Fig. 2. Walter and Leith Climate diagram of regional climate data based on CRU TS 3.22 climate records. MminT: Minimum Mean minimum Temperature, MmaxT: Maximum Mean maximum temperature, MAT: Mean annual temperature, MAP: Mean annual precipitation. Climate diagram is based on Walter and Lieth (1967).

sediment profile, dates at different depths were interpolated and extrapolated for each sample. The chronology detail of the sediment samples of the profile PTTL is provided in the supplementary material.

3.2. Palynological analysis

For the palynological analysis, standard procedure of acetolysis (Erdtmen, 1943) was followed to macerate the profile sediments. For each sample a minimum of 300 pollen grains were counted. The "Total Pollen Count" was calculated on the basis of the pollen of all taxa (arboreal and non-arboreal) along with other aquatic taxa and fern spores. To estimate "Pollen sum" the aquatic and fern taxa were excluded from the summations. A pollen diagram was constructed using the computer software TILIA version 2.0.2 (Grimm, 2004). On the basis of the variations of the major taxa of both arboreal and non-arboreal taxa the pollen diagram was further divided into pollen zones. These zones were drawn through stratigraphically constrained cluster analysis (CONISS, Grimm, 1987) using square root transferred data. These pollen zones are prefixed with the abbreviations after the name of PT TSo Lake as PTTL–I to PTTL–V.

3.2.1. Ordination analysis of palynological data

Principal Components Analysis (PCA) of the fossil pollen assemblage was carried out to study the relationships among the variables and to identify the principal component explaining the highest variance. The CANOCO computer programme version 5 (ter Braak and Šmilauer, 2012) was used for performing the PCA on the data. The pollen assemblages with more than 0.5% in abundance were considered for the PCA. This simplified the pollen matrix and made the methods consistent with cluster analysis carried out on the pollen data using CONISS (CONISS, Grimm, 1987).

3.2.2. Quantitative climate reconstruction

In the present study we also attempted quantitative climate reconstruction using transfer function methods (Birks, 1995; Birks et al., 2010). For this modern pollen–climate calibration was established and significant climate variable was reconstructed using fossil pollen record of PTTL. The reconstructed climatic variables were then supplemented with environmental geomagnetic and $\delta^{13}C$ Isotope data of the profile sediments. To establish modern pollen–climate relationships and subsequently for the development of transfer functions models, climatic variables viz., mean annual temperature (MAT), mean temperature of coldest month (MTCO), mean temperature of warmest month (MTWA) and mean annual precipitation (MAP) were taken into consideration. These climatic variables were interpolated for five modern pollen sites (moss cushion) collected from Tawang and west Kameng district of Arunachal Pradesh (see supplementary material). The interpolation was carried out using global land areas high-resolution climate data set of New et al. (2002). The weighted distance interpolation procedure was used for climate estimation to each modern pollen site after a reduction of all stations to the sea level (Guiot and Goeury, 1996).

Detrended correspondence analysis (DCA) was carried out to determine whether the pollen datasets along the climatic gradient follows linear–based or unimodal–based statistical methods (Birks, 1995). Based on the observed gradient length (< 2.5) our data showed linear response. Thus linear ordination approach, RDA was used along with the climatic variables to check its quantitative influence on the datasets. The Monte Carlo permutation tests (using 999 random permutations) were used to determine the statistical significance in the ordination. The forward modeling technique was used to determine significant climate variable which has unique influence on the distribution of pollen assemblages. All ordination analysis was carried out in programme CANOCO, version 5 (terBraak and Šmilauer, 2012). The method of partial least square regression (PLS) approach (terBraak and Juggins, 1993) was used to develop the pollen–climate transfer function for significant climate variable. The PLS model was verified using leave–one–out cross–validation procedure (Michaelsen, 1987; terBraak and Jugins, 1993) using PLS components to determine the optimum transfer function and to detect the samples with large residuals. The PLS model performance was assessed using statistical criteria such as root mean square error for prediction (RMSEP) and coefficient of determination (r^2) of observed versus predicted values. The number of

PLS–components included was selected on the basis of lowest RMSEP and highest r^2 between observed and predicted values (terBraak and Juggins, 1993; Berks, 1995, 1998). The sample specific error for reconstruction was done by applying 1000 bootstrap cycles. The quantitative climate reconstruction was carried out through transfer functions model developed in R version 3.3.0 (R Core Team, 2016) using the *rioja* package (Juggins, 2016).

3.3. Environmental magnetic measurements

For the mineral magnetic measurements the sediment samples were prepared using standard procedures detailed in Thompson and Oldfield (1986), Basavaiah and Khadkikar (2004) and Basavaiah (2011). Firstly each sample was oven dried at a temperature up to 40 °C overnight. Then these samples were crushed and packed in 8 cc cylindrical plastic holders and weighed. In the Environmental Magnetism Laboratory, Indian Institute of Geomagnetism, Navi Mumbai the samples were analysed for the mineral magnetic measurements. The high and low frequency magnetic susceptibility (χ_{LF} at 0.976 kHz and χ_{HF} at 1.6 kHz with units of $10^{-8}\,m^3/kg$) was measure on an AGICO MFK1 Kappabridge instrument; which helps to indicate the type and concentration of the magnetic minerals in the sample. Frequency-dependent susceptibility (FD%) [$(\chi_{LF} - \chi_{HF})x100/\chi_{LF}$] is considered to record the superparamagnetic (SP) ultrafine (~0.02 μm) ferrimgnetic minerals (e.g., magnetite) during soil formation. FD % probably also serves as a proxy for soil erosion (Thompson and Oldfield, 1986; Dearing et al., 1996). The Molspin spinner magnetometer was used to measure the Anhysteretic and isothermal remanent magnetizations (ARM and IRM) of the sediments. ARM was imparted in a DC bias field of 0.1 mT with a peak AF field of 100 mT. Susceptibility of ARM (χARM, $10^{-5}\,m^3/kg$) was calculated by dividing the ARM by the DC bias field. Saturation IRM (SIRM, $10^{-5}\,Am^2/kg$) was incorporated using a Molspin pulse magnetizer. The samples were normalized for differences in density by dividing each sample's weight. The S–Ratio was calculated from the SIRM and backfield IRM results based on the equation: S-Ratio = $IRM_{-0.3}$/SIRM (Bloemendal et al., 1992; Basavaiah and Khadkikar, 2004). It aids in distinguishing between high-coercivity magnetic minerals (e.g., hematite) from low-coercivity magnetic minerals (e.g., magnetite). To understand the relative variations in the amount of magnetite and hematite, the Soft IRM (SIRM - IRM_{-20}) and Hard IRM (SIRM - $IRM_{-0.3}$) were also calculated, respectively. The interparametric ratios such as ARM/SIRM and SIRM/χ_{LF} were calculated to measure the magnetic characteristics that are independent of magnetite concentrations, such as magnetic grain size and mineralogy. Independently these mineral magnetic parameters such as χ_{LF}, ARM and SIRM are basically representing a measure of magnetite concentration. The fraction of finer single-domain (SD) magnetite grains in the 0.02–0.5 μm size range are said to be dominant when there is an increase in the ARM/SIRM ratio which indicates decrease in the magnetic grain size. On the contrary low ARM/SIRM values indicate a large multi-domain (MD) magnetite component (0.5–10 μm size range). The MD component from the primary fine minerals present along with the fine SP and SD mode created by environmental transformations of Fe oxides as a result of pedogenesis, discern into a bimodal distribution. The low S-ratio and higher ARM/SRM ratio values are yielded by the SD grains contributed by the weakly magnetic hematite occurring in the sediments.

3.4. Carbon isotope analysis

The $\delta^{13}C$ isotope analysis of the profile sediments was carried out at the Physical Research Laboratory, Ahmadabad. About 1 gm of dry soil sample placed in a small quartz tube with an outer diameter 9 mm, along with pure CuO powder (Laskar et al., 2012) to analyze the soil organic carbon for stable isotopes measurements. This tube sealed with quartz wool, was evacuated, and heated at ~900 °C for ~1 h to produce CO_2. The cyogenical purification of this CO_2 was done over several steps and a stable isotope ratio mass spectrometer (GEO 20–20, Europa Scientific, UK) was used to measure its carbon isotopic composition ($\delta^{13}C$). The $\delta^{13}C$ measurements had an external precision better than ± 0.2‰ (Laskar, 2011; Laskar et al., 2012). An international standard solution of Oxalic acid II supplied by the National Bureau of Standards, used as a modern reference for ^{14}C dating, was used to measure the accuracy of the measurements. The average $\delta^{13}C$ (with respect to V–PDB) obtained is −17.7 ± 0.1‰, close to the internationally accepted value of −17.8‰ (Laskar, 2011; Laskar et al., 2012).

The metabolic processes through which Carbon is incorporated into plants control the $\delta^{13}C$ values of plant tissue (Faure, 1977; Faure and Mensing, 2004). The $\delta^{13}C$ values ranging from −23‰ to −34‰ with a mean value of −27‰ represent the plants following the Calvin cycle (C_3 plants: mostly plant on land) to metabolize CO_2. Whereas the $\delta^{13}C$ values between −9‰ and −23‰ having a mean of −13‰ indicate occurrence of the Hatch–Slack pathway-following plants (C_4 plants: aquatic, desert and salt marsh plants as well as tropical grasses) (Faure, 1977; Faure and Mensing, 2004). Thus in the present carbon isotopic study was carried out to examine the variations in $\delta^{13}C$ of the PTTL profile sediments. Primarily to understand the productivity of the C_3 and C_4 plants in the PTTL sediments and their resemblance with the pollen and magnetic susceptibility records.

4. Results

4.1. Palaeo–vegetation history

The chronology of the sediment profile based on linear regression showed that it covers the last 8010 cal yr BP, confirming that these sediments covers time span since early Holocene. So the present fossil records represent the vegetation and climate records since early Holocene (see supplementary material). Based on the CONISS analysis on percentage pollen data, five zones viz., PTTL – I to PTTL – V were established to represent the major phase of vegetation change (see supplementary material). The vegetation changes in each pollen zone are described in details in the supplementary material.

4.1.1. Ordination analysis – PCA

The PCA resulted in explaining 65.37% of total variance for the first principal component (PC1) retained. The species distribution in the subsurface sediment samples was determined by the important factors displayed by the PC1. The significant fluctuation in species abundance occurred within the sediment around 4.2 cal yr BP that is also marked by variation in PC1. Most of the species distributed at each depth are represented at this point of change in PC1 (Fig. 3). The species component score of the complete sediment profile includes taxa namely Magnoliaceae, *Tsuga*, *Rhododendron*, Juniper, *Pinus*, *Abies*, *Larix*, *Betula*, *Corylus*, *Alnus*, *Quercus* in increasing order. The PC2 explained a total variance of 25.37% where the highest scores displayed by Magnoliaceae and *Tsuga*. Thus PC1 included almost all significant species in the sediment profile but a sudden but stepwise change in species abundance is recorded after Pollen zone PTTL-II around 4.2 cal yr BP.

4.1.2. Reconstructed climatic parameter

In RDA, we found MTCO is the most promising climatic variable based on forward modeling approach. The constrained ordination using RDA with pollen and MTCO explained variance of 40.83% and 32.10% in Axis 1 and Axis 2 respectively (see supplementary material). The climate variable, MTCO was used to develop transfer function model. The performance of transfer function models for MTCO showed that the second component to be the best performing model. It showed the lowest value (4.4296) of RMSEP and moderate value (0.646) of r^2 between observed and predicted MTCO (see supplementary material). The successful validation of the transfer function models for MTCO based on

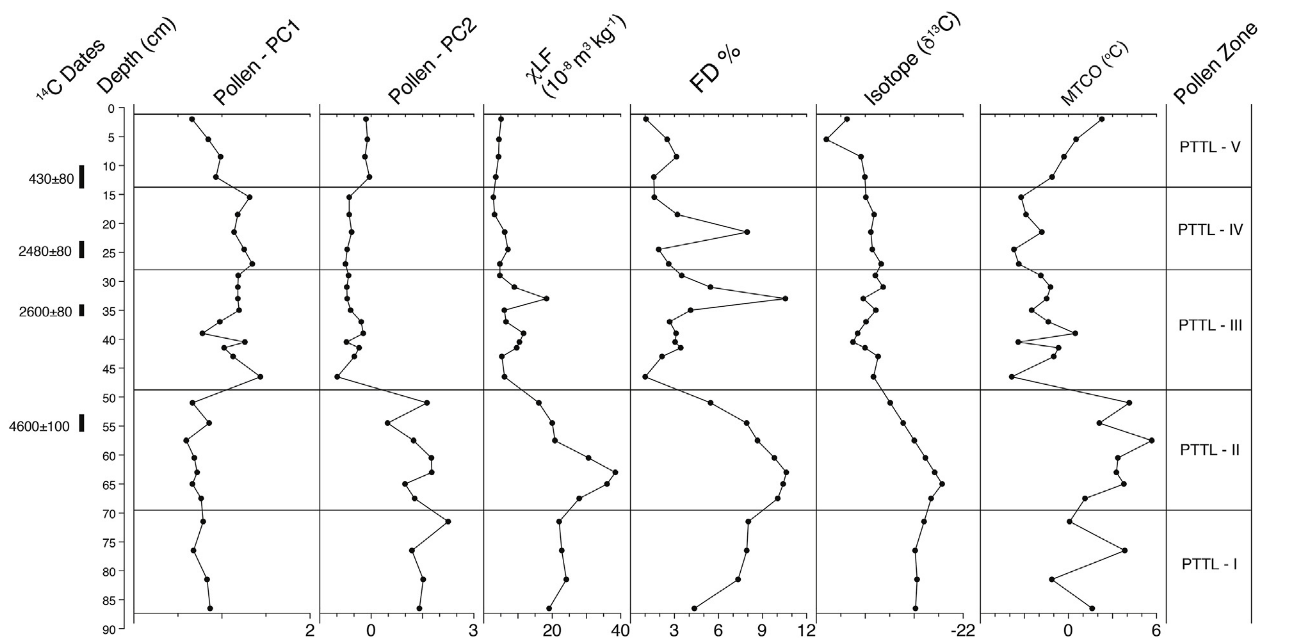

Fig. 3. Composite diagrammatic representation of PC1, PC2, Environmental geomagnetism parameters, $\delta^{13}C$ Isotope and MTCO variations in the sediment profile.

standard statistical criteria (Birks, 1995) shows its prospect for quantitative reconstruction of in the present study. This leads to the reconstruction of MTCO since 8010 cal yr BP for PTTL fossil pollen profile from Tawang, Arunachal Pradesh (Fig. 3).

5. Discussion

5.1. Palaeo-environmental changes at PT Tso Lake, Eastern Himalaya

The entire sediment profile records high occurrence of tree taxa and discrete variation in the fern-spore counts. The lower pollen zones (PTTL–I and PTTL–II) record fewer pollen counts of different taxa but tree species such as Magnoliaceae, *Tsuga*, *Larix*, are dominant. But we recorded fern spore in excessive numbers in these zones in comparison to overlying zones. These sub-tropical-temperate species occupy up to ~4814 cal yr BP indicating less cold and humid conditions near PT Tso Lake. Similar Himalayan moist temperate forests are found in Eastern Himalaya in modern times. These modern evergreen forests are comprised of conifers or Oaks, or a mixture of both (Champion and Seth, 1968a).

The key elements of the present day Himalayan moist temperate forests are *Tsuga dumosa*, *Abies densa* with *Quercus pachyphylla* in the upper aspect, whereas *Tsuga*, with *Q. lineata* and *Q. lamellosa* in the lower aspect (Champion and Seth, 1968a). The Eastern Himalayan mixed coniferous forests a subdivision of Himalayan moist temperate forests, are found at altitudes between 2300 and 3000 m. They are occupying regions such as the present day Sikkim Himalaya (not the outer most ranges), Mishmi hills, N.E.F.A. (North-East Frontier Agency, now known as Arunachal Pradesh) and westwards into Nepal (Champion and Seth, 1968b). The taxa such as *Tsuga dumosa*, *Abies densa*, *Q. pachyphylla*, *Q. lineata*, *Acer campbellii*, *Magnolia campbellii*, *Betula utilis*, *Rhododendron arboreum*, *R. grande*, *Symplocos phyllocalyx*, etc, along with abundant Ferns (Champion and Seth, 1968b) are the constituent flora of these forests presently.

Thus the present day Eastern Himalaya mixed coniferous forests type was present around PT TSo Lake and less cold and humid prevailed until ~4814 cal yr BP. But the temperature was possibly higher than the present and also in the overlying zones (PTTL III-V) of the sediment profile. The taxa dominant in zones PTTL-I and II are now confined to lower altitudes i.e., between 2300 and 3000 m in Tawang and other parts of the Eastern Himalaya.

The mineral magnetic data supports the interpretation of the vegetation vis-à-vis climate conditions prevailing around PT Tso Lake. The overall magnetite content was more along the lines of this increase in available moisture in the sediments. There was a possible increase in the organic input as the magnetic trends increased in these pollen zones with low pollen counts (PTTL- I and PTTL-II). The domination of mixed vegetation was also recorded in the $\delta^{13}C$ isotope which signaled the presence of both C_3–C_4 plants in the same period. The reconstructed temperature record fluctuates but has higher temperatures than overlying zones.

The next zone PTTL–III a significant change in the vegetation is recorded in the sediment profile. The taxa that mostly occur in temperate to sub alpine belts were dominant in this zone. These included plants such as *Quercus* (19–54%), *Betula* (6–12%), *Larix* (5–10%), Ericaceae (1–16%), *Alnus* (6–12%), which thrived in the Tawang region, between 4195 and 2527 cal yr BP; but during this period the temperate taxa such as Magnoliaceae, *Tsuga* and the ferns were reduced significantly. The forest type occupying the region during this period varied between modern day Himalayan dry temperate forests to subalpine forest vegetation. The former is found around 3000 m asl as open evergreen forest with scrub undergrowth having both coniferous and broad leaved species (Champion and Seth, 1968a). These forests have *Larix griffithiana* growing on moraine soils at 3000–4000 m along with *Abies*, *Picea* etc, reaching from the moist zones and *Juniper wallichiana* from higher altitude (Champion and Seth, 1968a). Whereas the subalpine forests that are presently comprised by *Betula* and *Abies densa*, Blue pine, and *Rhododendrons* in Eastern Himalayas above 3000 m (Champion and Seth, 1968a).

Later these taxa vary significantly indicating less cold and humid conditions in the early part of the zone PTTL-III. And further there is shift towards cold and dry environment in the later part of this zone. The sudden decrease of Magnoliaceae, *Tsuga* and the ferns also point towards a transition in to less moist conditions. Although *Quercus* is the dominant element in this zone but it fluctuated throughout the zone. This variation in the pollen taxa is also observed in PC1 record in this zone (Fig. 3). It can probably be considered as an extra-local element or also coming from lower elevation, when dryer conditions cause stronger winds that brought in excessively produced Oak pollens. The mineral magnetic parameters such as SIRM, ARM, FD% and S–ratio indicate a low magnetite content and overall drier environment around the sediments and higher HIRM values than lower zone showed a rise in hematite contents (see supplementary material). Similarly the $\delta^{13}C$ data indicates that C_3 plants mostly dominate this zone. The zone PTTL-III witnessed a cod dry phase and the palynological and mineral magnetic data synchronously change with the changes in the reconstructed MTCO, which show a remarkable fall in temperature in the region (Fig. 3).

The zones PTTL–IV and PTTL–V have ages ranging between 2336 and 1240 cal yr BP to 906 cal yr BP and present. In these zones the MTCO fluctuate and gradually rise after 906 cal yr BP. In the early part of the PTTL–IV zone the environmental magnetic data indicates some magnetite content. But later most of the parameter values signify higher hematite content upto 906 cal yr BP. The $\delta^{13}C$ values during 2527–906 cal yr BP signified the occurrence of C_3 vegetation and the values were mostly constant. The pollen data recorded a decrease in the counts towards the upper part of the profile and similar vegetation continues as in PTTL–III. In the zone PTTL–V (906 cal yr BP to present) the sub alpine forests replaced the dry temperate forests dominating in PTTL–IV. Such sub alpine forests are also presently known as the *Rhododendron* forests in Arunachal Pradesh (N.E.F.A.). These *Rhododendron* forests have taxa such as *Abies densa*, *Juniper wallichiana*, *Rhododendron*, *Betula utilis*, *Salix wallichiana*, *Polygonum* spp. growing in the eastern Himalayas above 3000 m along with *Larix griffithiana* and *Picea spinulosa* presently (Champion and Seth, 1968b). The *Rhododendron* and *Larix* replace Oaks by the end of zone PTTL–V. Probably the anthropogenic activities such as cultivation and farming in the region have caused this change in the vegetation. The Oak (*Quercus* spp) is extensively utilized by the local tribes (such as *Monpas of Tawang*). They use Oak leaves as manure in cultivation and Oak wood for firewood even today (Biswal, 2006). The *Monpa* tribe also trades the leaves of *Quercus griffithii* (local name *paisang*) with the *Brokpa*, a yak breeding highlander community located in Tawang and West Kameng districts. The *Brokpa* tribes live in higher altitudes and move down to lower altitude during peak winters, to exchange *paisang* leaves and wood with yak-based food products to *Monpas* cultivating *paisang* at lower altitudes till present times (Singh et al., 2015). The *Monpa* tribe is said to have migrated around fourth century (~1650 cal yrs BP) from the Tibet regions (Chakravarty, 1973; Norbu, 2015). Hence these Oak cultivation practices could have been continuing since their occupancy or probably earlier by other inhabitants of the region. Human occupancy in Arunachal Pradesh has been reported since the Neolithic period. Neolithic age stone tool were found from Parsi parlo, in Kurung Kumey district and Daporijo, in Upper Subansari district towards the east of present study site (Dikshit & Hazarika, 2011–12). Thus the presence of humans and their impact on the vegetation of this region or surrounding areas since the Neolithic period could be one of the factors influencing the environmental changes and vice-versa. Though the direct impact of environmental changes and palaeoclimatic fluctuation on the past human populations of Arunachal Pradesh have not been successfully recorded.

A drastic change in the vegetation vis–à–vis climatic conditions occurred around the PT Tso Lake between ~8000 and 906 cal yr BP. The climate around the lake became more cold and dry as signaled by the multi–proxy data. The strengths of the southwest monsoon in the region probably altered during Holocene and similar conditions still persist. But a sudden change in the data had occurred around ~4.2 cal yr BP implicating the impact of the change on the proxy record. After this ACC event the vegetation vis-à-vis climate did not revert back the conditions occurring prior to the event. The multi-proxy records and the temperature reconstruction clearly indicated this strong change in the environmental conditions around the PT Tso Lake. The human impact on the vegetation may be creating a parallel impact and possibly causing the degradation of the vegetation. Additionally the climate had probably influenced the environment and the lake catchment in equal measure, as recorded by various proxies These Holocene proxy records establish the sensitivity of the region towards climate change. Undoubtedly an ACC event occurred around the high altitude lake of Eastern Himalaya and surrounding regions of Tawang.

The reduction in the strength of the southwest monsoon in the Eastern Himalaya region and parts of Northeast India during the 4.2ka (ACC) event was also simultaneously impacting the western parts of India and Western Himalaya region. Western Himalaya and Central Himalaya have recorded similar records of 4.2ka (ACC) events where cold and dry episodes have impacted the vegetation vis-à-vis climate conditions. Stalagmite from Sainji cave deposits in western Himalaya recorded a pattern of reduction in precipitation during the millennia from 4000 cal yr BP to ~3000 cal yr BP with the lowest precipitation at ~3200 cal yr BP (Kotlia et al., 2015). In the Tso Moriri Lake, northwestern Himalaya a cold and arid phase from ~4350 to 3450 cal yr BP in the region was recorded (Dutt et al., 2018). The Phulara palaeolake in the Kumaun Himalaya also recorded rising $\delta^{13}C$ and variable magnetic susceptibility values around the 4.2ka event (Kotlia et al., 2010). Similarly weakening of the SW monsoon was recorded in the central Himalaya resulting into an arid phase around 4000 cal yr BP (Phadtare, 2000). Pollen record from Surinsar Lake, Jammu, north-western Himalaya suggested a weakening of the monsoon strength and a cold and arid phase during 4000 to 2100 cal yr BP in the region (Trivedi and Chauhan, 2009). Similarly the Karsandi palaeolake record from Rajasthan western India records prevalent dry conditions during 4400 cal yr BP to ~3900 cal yr BP (Dixit et al., 2018). This phase of aridity had impacted the population dwelling in the region of Thar Desert and they shifted towards eastern margins, as higher palaeolake levels were observed in the east where more archeological evidences persisted (Dixit et al., 2018). Thus this change in climatic conditions and monsoon strength also impacted the human civilization during the late Mid Holocene in several regions in India and globally.

5.2. The Holocene ACC events: the impacts recorded and societal damage caused globally

The ACC events during the Holocene were simultaneously recorded in Northern hemisphere and were creating major societal impacts on various civilizations of Africa, Pan Asia or the old world cultures (Redman et al., 2007). A high resolution $\delta^{18}O$ of calcite from a speleothem of Mawmluh Cave (25°15′44″N, 91°52′54″E, elevation 1290 m) at Cherrapunji, Meghalaya, was spanning 3600 to 12,500 years BP (Berkelhammer et al., 2012). Cherrapunji has very high annual average precipitation ~11,000 mm, making it one of the wettest place on the planet. A major part (70%) of the rainfall occurs during the summer monsoon months i.e., June–September (Murata et al., 2007). The stalagmite witnessed highest isotopic enrichment between 4071 BP (± 18 years) and 3888 BP (± 22 years) for about 183 years. This record is close to the 4.2 cal yr BP. The ACC event was probably caused by changes is monsoonal dynamics in the region. Indian summer monsoon (ISM) anomalies have been recorded in Dandak cave from east central India, which observes a cyclic pattern of the ISM similar to Gleissberg solar cycle and multi–decadal sea surface temperature variability in the North Atlantic Oscillation (AMO) between 600–1550 CE. Similar isotope records from Renella Cave (Alpi Apuane, central Italy) in southern Europe, have recorded the 4.2 ACC events and shift towards dryer and colder conditions (Drysdale et al., 2006).

5.2.1. Damage caused to various civilizations globally

The societal impact on some major civilizations such as the Indus Valley civilization, Mesopotamia, of the Bronze Age has been discussed below along with few other global records of the 4.2 ACC events. Some of these sites along with few records mentioned in composite studies of the records of indicating impact of the ACC events on various civilizations of a region and environmental changes (Cold/Dry conditions) caused are given in Figs. 1 and 4.

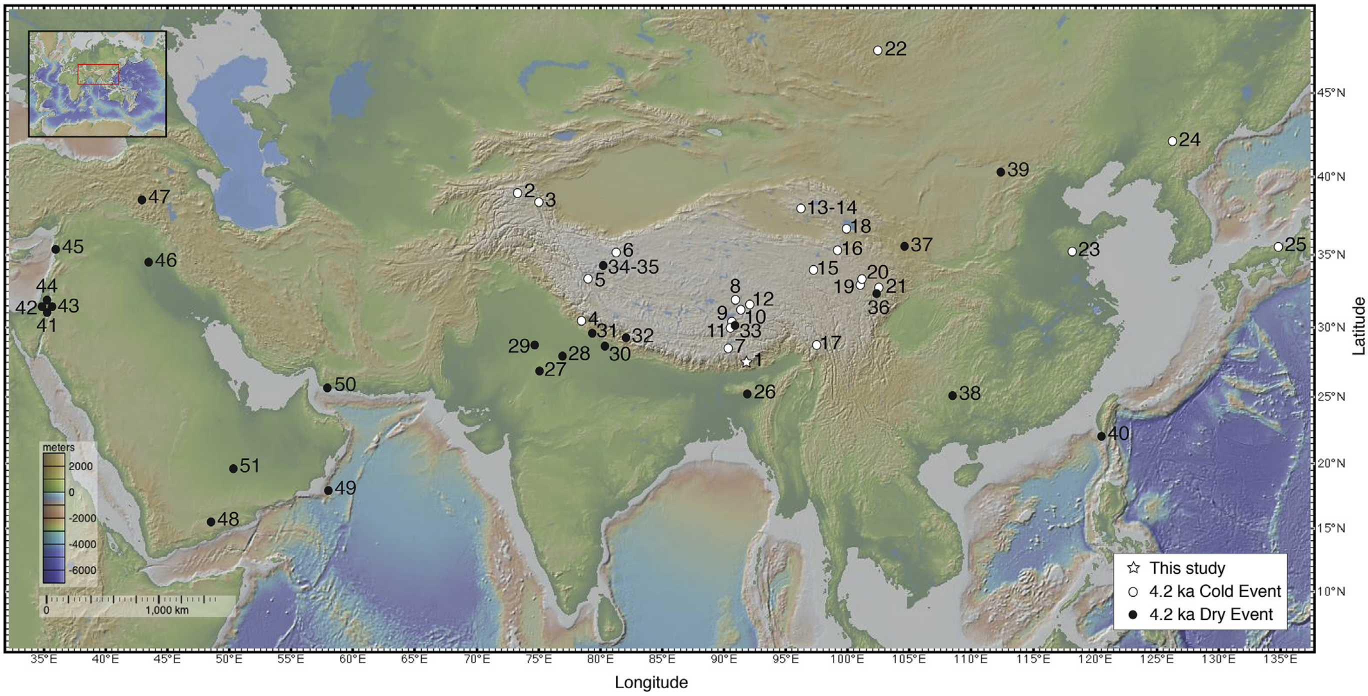

Fig. 4. Map showing present study site along with 4.2ka cold and dry event records. Details of the location are 1 PTTL (Present study site); 2 Lake Karakul, Tajikistan (Mischke et al., 2010a); 3 glacier record of Muztag Ata and Kongur Shan (Seong et al., 2009); 4 Garhwal Himalayan peat, India (Phadtare, 2000); 5 Bangong and Sumxi Co (Gasse et al., 1996); 6 Guliya ice core (Thompson et al., 1997); 7 Chen Co (Zhu et al., 2009a); 8 Zigetang Lake (Herzschuh et al., 2006); 9 Nam Co (Zhu et al., 2009b); 10 Cuoe Lake (Wu et al., 2006); 11 central Tibetan peats (Wang and Fan, 1987); 12 Ahung Co (Morrill et al., 2006); 13 Dunde ice core pollen (Liu et al., 1998); 14 Dunde ice core δ18O (Yao and Thompson, 1992); 15 Lake Koucha (Mischke et al., 2008); 16 Lake Kuhai (Mischke et al., 2010b); 17 Naleng Co (Kramer et al., 2010); 18 Lake Qinghai (Shen et al., 2005); 19 Nianbaoyeze Shan peats (Schlü;tz and Lehmkuhl, 2009); 20 Lake Ximencuo (Mischke and Zhang, 2010); 21 Hongyuan peat (Yu et al., 2006); 22 Ugii Nuur Basin (Schwanghart et al., 2008); 23 Yishu River Basin (Gao et al., 2007); 24 Jinchuan (Jiang et al., 2008); 25 Tougou-ike Lake (Kato et al., 2003); 26 Mawmluh cave (Berkelhammer et al., 2011, 2012); 27 NW-India (Enzel et al., 1999; MacDonald, 2011); 28 Kotla Dahar (Dixit et al., 2014); 29 Karsandi palaeolake (Dixit et al., 2018); 30 Phulara palaeolake (Kotlia et al., 2010); 31 Sainji Cave (Kotlia et al., 2015); 32 Rara Lake (Nakamura et al., 2016); 33 Tibetan Plateau (Mügler et al., 2010); 34 Tibetan Plateau (Gasse and VanCampo, 1994); 35 Tibetan Plateau (Wei and Gasse, 1999); 36 Hongyuan Bog (Hong et al., 2003); 37 W Loess Plateau (An et al., 2005); 38 Dongge cave (Wang et al., 2005); 39 Daihai lake (Peng et al., 2005); 40 Tung-Yuan Pond (Yang et al., 2011); 41 Dead Sea (Migowski et al., 2006); 42 Soreq Cave (Bar-Matthews et al., 2003); 43 Dead Sea (Frumkin et al., 2001); 44 Dead Sea (Enzel et al., 2003); 45 Syrian coast (Kaniewski et al., 2008); 46 Tell Leilan (Weiss et al., 1993); 47 Lake Van (Lemcke and Sturm, 1997); 48 High Plateau of Yemen (Wilkinson, 1997); 49 Arabian sea (Gupta et al., 2003); 50 SE Arabia (Parker et al., 2006); 51 NE Rub'alNKhali desert (Parker et al., 2004). Note: Location 2 to 25 represent cold 4.2ka event and locations 26 to 51 represents dry 4.2ka event.

5.2.1.1. Indus valley civilization. The Harappan civilization flourished along the Indus valley in Pakistan and across the NW India between ~9000 and 3000 cal yr BP (Marshal, 1931; Enzel et al., 1999; Possehl, 2002). This urbanized population of the Bronze Age expanded during the Mid Holocene intensification on the Indian summer monsoon (McDonald, 2011; Possehl, 2002; Sarkar et al., 2016) i.e., during the Early Harappan phase (~8–6.5 cal yr BP) (Sarkar et al., 2016). But the de–urbanization and abandonment of major cities occurred followed by the collapse of the Harappan Civilization occurred around 3.9 cal a BP (Possehl, 1997; Redman et al., 2007 and references there in). This decline has been attributed to several causes such as Aryan invasion, catastrophic floods or droughts, variations in the monsoon dynamics and resulting river flow changes, reduction in trade etc., (McDonald, 2011; Sarkar et al., 2016 and references there in). Proxy based evidences such as fossil pollen (Singh, 1971; Singh et al., 1972, 1990; Possehl, 1997), $\delta^{18}O$ record of gastropod aragonite (Dixit et al., 2014), animal teeth bone phosphate (Sarkar et al., 2016), archaeobotanical, geochemical, and stable carbon isotope ($\delta^{13}C$) (Pokharia et al., 2017), U–Pb zircon dating (Clift et al., 2012), fluvial morpho–dynamics (Giosan et al., 2012), from western India and $\delta^{18}O$ of planktonic foraminifera *Globigerinoides ruber,* from off Pakistan, Arabian sea (Gupta et al., 2003), have recorded the influence of the 4.2 cal yr BP ACC event in the region. Although there is speculation regarding the impact of the 4.2 aridification event or reduced intensity of Indian summer monsoon as a causative of the decline of the Harappan civilization (Enzel et al., 1999; Weiss and Bradley, 2001).

5.2.1.2. Mesopotamia. The agricultural lands of rain fed Subir of Northern Mesopotamia civilization on the Habur plains and irrigation based agriculture of Sumer and Akkad in southern Mesopotamia flourished under the rule of Sargon of Akkad (Weiss et al., 1993) from 2300 to 2200 B.C. For ~100 years the imperial Akkadian empire had controlled the socio political military set up and conducted intense agriculture practices in the gradually degrading climate (Weiss et al., 1993). Between ~2200 and 1900 B.C. large populations from Northern Mesopotamia, Habur plains abandoned these desertified region and moved into southern Mesopotamia (Weiss et al., 1993; Weiss, 2000). After 100 years the prosperous Akkadian empire abruptly collapsed at ca. 4170 ± 150 cal yr BP (Postgate, 1992; Weiss et al., 1993; deMenocal, 2001). Intense desertification due to aridity, wind turbulence, dust veil, decreased agricultural productivity in Habur plain and abrupt climate change evidences were found in Tell Leilan stratified sediments. Evidence of volcanic tephra layers of Tell Leilan was followed by phase of aridity and sudden climate change in Habur plain. Excessive abandonment in North led to the building of Repeller of Amorites, a 180 km long wall across central Mesopotamia to check the influx of refugees to south (Weiss et al., 1993). The Low flow in Euphrates and Tigris rivers, increased population, diminishing political control and abrupt climate change resulted in the final collapse of the Akkadian empire (Weiss et al., 1993).

5.2.1.3. Other global records. Many regions of the northern hemisphere such Egypt, Tibet, Nepal, China, have been impacted severely by the same ACC events (Redman et al., 2007 and references there in; Liu and Feng, 2012). The ancient Kingdom of Egypt had civil conflicts after the end of the regimes of Userkaf and Sahure around 4400 cal yr BP. The large building projects of the Fourth Dynasty weakened and ended the treasury of the Kingdom. The Old Kingdom faced several decades of famine and strife during the severe drought that occurred between 4200 and 4150 cal yr BP causing the final collapse of the Kingdom (Dalfes et al., 1997; Stanley et al., 2003; Drysdale et al., 2006; Liu and Feng, 2012).

In Tibetan Plateau a cold event was recorded in the lake and peat sections, ice cores and glacial remains during the Holocene around 4.2 cal yr BP. A large area of the Tibetan plateau and surrounding regions were impacted and this ACC event recorded at many sites (Mischke and Zhang, 2010). The cold event prolonged for almost a millennium in the western and central regions and for several hundred years in the eastern region. A temporary trans-regional climate response in the Tibetan Plateau had probably influenced each catchment of the lake sediment and peat accumulation resulting from the end of the Holocene "climatic optimum". The end of old and advent of new Chinese Dynasties happened simultaneously to these cold events after 4.2 cal yr B.P (Fig. 1) thus impacting the social system of eastern China (Mischke and Zhang, 2010).

A study from Lake Rara, western Nepal was based on the analysis of redox sensitive elements (Mn/Ti and Mn/Fe) and organic matter properties (TOC, d13C, and C/N) of the lake sediments, recorded the Indian summer monsoon variation particularly focusing on the 4.2 ka event (Nakamura et al., 2016). The environmental reconstruction from Lake Rara concluded that surface processes and soil dynamics in the catchment, were driven by hydroclimate variability in this Himalayan region of Nepal. The low Mn/Ti and Mn/Fe recorded in the lake sediments between 4.2 and 3.7 ka signaled an interval of weak summer monsoon intensity. This weak summer monsoon interval at around 4 ka coincided with the 4.2 ka event recorded elsewhere (Nakamura et al., 2016).

A detailed review of climate proxy records and archeological literature of climate variations and cultural collapse in China during ~8500–~3500 cal yr B.P. was compiled by (Liu and Feng, 2012). A major part of China was impacted by the ACC event at ~4000 cal yr B.P which is a much documented occurrence. Excluding Henan Longshan Culture, the collapse of six out of the seven Neolithic cultures, in China at ~4000 cal yr B.P was recorded and well documented. This collapse of cultures resulted in reduction of archeological sites, lowering of quality of artifacts, disappearance of advanced architectures and change into pastoral or agro–pastoral adaptations in agriculture, which were the major societal impacts documented.

5.2.2. The Holocene ACC events: the probable causes

The occurrence of the Holocene ACC event has been reported throughout the northern Hemisphere for which many causes have been given and impacts reported globally (Roland, 2012). The primary factor causing these events was speculated to be the change in the monsoon dynamics over the Indian subcontinent. The ISM possesses a complex and spatially heterogeneous nature. An anomaly in the ISM around ~4000 cal yr BP has been recorded in the Kotla Dahar paleolake (Dixit et al., 2014) in northwest and Mawmluh cave (Berkelhammer et al., 2012) in eastern India. This peculiar anomaly in the ISM dynamics has be attributed to a coupled feedback of Indian Ocean Dipole (IOD), Sea surface temperature gradients in Eastern tropical pacific and changes in ENSO activity (Berkelhammer et al., 2012; Dixit et al., 2014). A forcing is generated in the higher latitudes of the Northern Hemisphere (i.e., the North Atlantic) (Bond et al., 1997, 2001; Hong et al., 2003) or due to variability in the solar insolation (McDonald, 2011) creates these coupled feedbacks impacting the ISM. The likely change in the ISM strength created cool and arid conditions further initiating fluctuation in mid-latitude westerlies (Ding and Wang, 2005; Krishnan et al., 2009). Thus causing dry extra–tropical air to enter the monsoon system and form a comprehensive feedback loop of ISM and westerlies leading to further weaker monsoon (Berkelhammer et al., 2012). Such cool and arid conditions in the Holocene occurred around 4.2 cal yr BP and were recorded in regions around the present study area such as Cherrapunji in north–east India (Berkelhammer et al., 2012), Tibet (Hong et al., 2003; Mischke and Zhang, 2010) and China (Liu and Feng, 2012). It is thus forming an imperative link of the various proxies responding to changes on the monsoonal patterns, possibly due to a circum-global pressure anomaly generated by the feedback system (Berkelhammer et al., 2012). Hence similar signal of ACC event and changes in the ISM strength are generated by the proxy records in NE India and surrounding region. Consequently this coupled impact on vegetation vis-à-vis climate in the Eastern Himalaya during the Holocene is being recorded in the present multi proxy analysis.

6. Conclusions

The high altitude region of the PT Tso Lake, in Tawang, in the Eastern Himalaya recorded environmental changes around 4.2 cal yr BP. There were episodes of monsoon intensification during the Mid Holocene, followed by low temperatures and high aridity conditions during the ACC event period of the early Late Holocene. These climate fluctuations in the Eastern Himalaya were recorded in multi-proxy records of palynological, carbon isotope and mineral magnetism of sediments at the catchment of PT TSo Lake. Such ACC events have been recorded globally and have impacted major civilizations in China, Tibet, Western India, Mesopotamia, Egypt and many other regions. The significance and impact of such ACC events on the human society in the past and also in the coming future need to be further identified. Longer palaeo–climatic reconstructions based on higher resolution proxy records from the populous Eastern Himalaya are needed in future to strongly establish the climatic variations and it societal impact during the entire Holocene.

Acknowledgements

The authors are grateful to Prof. Sunil Bajpai, the Director, Birbal Sahni Institute of Palaeosciences, Lucknow, India, for the help and support during the preparation of this manuscript and study carried out at BSIP (BSIP/RDCC/Publication No:75/2017-18). The Author NM is thankful to DST. (D.S.T.–WOS–A scheme–SR/WOS–A/ES–18/2014), New Delhi, Govt. of India and CSIR (SRF–Direct–grant no 09/528/(0017)/2012/EMR–I) for the financial support they provided her for this study and during the preparation of this manuscript. The study was also supported by DST. sponsored project No SR/S4/ES-15/2002 and authors are thankful. The authors are also thankful to Indian Institute of Geomagnetism Navi Mumbai for the support provided during the mineral magnetism analysis. The authors are also thankful to the Physical Research Laboratory Ahmadabad, for the due help and support during the isotopic analysis and sediment dating. The Tawang forest division also kindly helped and supported during author SKS the collection of the sediment profile and we shall be ever grateful to the authorities. Authors are thankful to Cristina Robbins for the help and suggestions for the final version of this manuscript. We are thankful to the two reviewers for their comments to improve this manuscript. The authors also thank the guest Editor for his valuable suggestions and inputs in the final version of this manuscript.

Appendix A. Supplementary data

Supplementary data to this article can be found online at https://doi.org/10.1016/j.quaint.2018.09.027.

References

An, C., Tang, L., Barton, L., Chen, F., 2005. Climate change and cultural response around 4000 cal yr BP in the western part of Chinese Loess Plateau. Quat. Res. 63 (3), 347–352.

Baishya, A.K., Balodi, B., Pal, G.D., 2002. Floristic diversity of Arunachal Pradesh an overview. In: In: Sundriyal, R.C., Singh, T., Sinha, G.N. (Eds.), Arunachal Pradesh: Environmental Planning and Sustainable Development, vol. 16. Himavikas Occasional Publication, pp. 173–206.

Bar-Matthews, M., Ayalon, A., Gilmour, M., Matthews, A., Hawkesworth, C.J., 2003. Sea land oxygen isotopic relationships from planktonic foraminifera and speleothems in the Eastern Mediterranean region and their implication for paleorainfall during interglacial intervals. Geochem. Cosmochim. Acta 67 (17), 3181–3199.

Basavaiah, N., 2011. Geomagnetism: Solid Earth and Upper Atmosphere Perspectives. Springer, The Netherlands, pp. 291–386.

Basavaiah, N., Khadkikar, A.S., 2004. Environmental magnetism and paleomonsoon. J. Ind. Geophys. Union 8, 1–77.

Berkelhammer, M., Sinha, A., Stott, L., Cheng, H., Pausata, F.S.R., Yoshimura, K., 2012. An abrupt shift in the Indian monsoon 4000 years ago. In: In: Giosan, L. (Ed.), Climates, Landscapes, and Civilizations, vol. 198. American Geophysical Union Geophysical Monograph, pp. 75–87.

Berkelhammer, M.B., Sinha, A., Cheng, H., 2011. Indian Monsoon Failure during the 4.2 K Event. AGU Chapman Conference on Climates, Past Landscapes and Civilisations, Santa Fe, New Mexico.

Bhattacharyya, A., Chaudhary, V., 2003. Late–summer temperature reconstruction of the Eastern Himalayan Region based on tree–ring data of *Abies densa*. Arctic Antarct. Alpine Res. 35 (2), 196–202.

Birks, H.J.B., 1995. Quantitative palaeoenvironmental reconstructions. In: Maddy, D., Brew, J.S. (Eds.), Statistical Modelling of Quaternary Science Data. Quaternary Research Association, Cambridge, pp. 161–254.

Birks, H.J.B., 1998. Numerical tools in palaeolimnology – progress, potentialities, and problems. J. Paleolimnol. 20, 307–332.

Birks, H.J.B., 2010. Numerical methods for the analysis of diatom assemblage data. In: J, P., Stoermer, E.F. (Eds.), The Diatoms – Applications for the Environmental and Earth Sciences Smol. Cambridge University Press, Cambridge, pp. 23–54.

Biswal, A., 2006. Mystic Monpas of the Tawang Himalaya. Indus Publishing Company, New Delhi.

Blaauw, M., 2010. Methods and code for 'classical' age-modelling of radiocarbon sequences. Quat. Geochronol. 5, 512–518.

Bloemendal, J., King, J.W., Hall, F.R., Doh, S.J., 1992. Rock magnetism of Late Neogene and Pleistocene deep-sea sediments: relationship to sediment source, diagenetic processes, and sediment lithology. J. Geophys. Res. 97, 4361–4375.

Bond, G.C., Kromer, B., Beer, J., Muscheler, R., Evans, M., Showers, W., Hoffmann, S., Lotti–Bond, R., Hajdas, I., Bonani, G., 2001. Persistent solar influence on North Atlantic climate during the Holocene. Science 294, 2130–2136.

Bond, G.C., Showers, W., Cheseby, M., Lotti, R., Almasi, P., deMenocal, P., Priore, P., Cullen, H., Hajdas, I., Bonani, G., 1997. A Pervasive millennial-scale cycle in North Atlantic Holocene and glacial climates. Science 278, 1257–1266.

Booth, R.K., Jackson, S., Forman, S., Kutzbach, J., Bettis III, E., Kreigs, J., Wright, D., 2005. A severe centennial –scale drought in midcontinental North America 4200 years ago and apparent global linkages. Holocene 15, 321–328.

Chakravarty, L.N., 1973. Glimpses of the Early History of Arunachal. Directorate of Research, Government of Arunachal Pradesh, Itanagar, Arunchal Prasdesh, India.

Champion, H.G., Seth, S.K., 1968a. General Silviculture for India. Natraj Publishers, Dehradun, India.

Champion, H.G., Seth, S.K., 1968b. A Revised Survey of Forest Types of India. Natraj Publishers, Dehradun, India.

Chen, Z.Y., Wang, Z.H., Schneiderman, J., et al., 2005. Holocene climate fluctuations in the Yangtze delta of eastern China and the Neolithic response. Holocene 15, 915–924.

Clift, P.D., et al., 2012. U –Pb zircon dating evidence for a pleistocene Sarasvati river and capture of the Yamuna river. Geology 40, 211–214.

Cosford, J., Qing, H.R., Eglington, B., et al., 2008. East Asian monsoon variability since the mid-Holocene recorded in a high resolution absolute-dated aragonite speleothem from eastern China. Earth Planet Sci. Lett. 275, 296–307.

Cullen, H., deMenocal, P., Hemming, S., Hemming, G., Brown, F., Guilderson, T., Sirocko, F., 2000. Climate change and the collapse of the Akkadian empire: evidence from the deep sea. Geology 28, 379–382.

Dalfes, H.N., Kukla, G., Weiss, H., 1997. Third Millennium B.C. Climate Change and Old World Collapse. NATO ASI 1. Springer, New York (49).

Dearing, J.A., Hay, K.L., Baban, S.M.J., Huddleston, A.S., Wellington, E.M.H., Loveland, P.J., 1996. Magnetic susceptibility of soil: an evaluation of conflicting theories using a national data set. Geophys. J. Int. 127, 728–734.

deMenocal, P.B., 2001. Cultural responses to climate change during the late Holocene. Science 292, 667–673.

Dikshit, K.N., Hazarika, M., 2011-12. The Neolithic cultures of northeast India and adjoining regions: a comparative study. J. Ind. Ocean Archaeol. 7 & 8, 98–148.

Ding, Q., Wang, B., 2005. Circumglobal teleconnection in the northern hemisphere summer. J. Clim. 18 (17), 3483–3505.

Dixit, Y., Hodell, D.A., Petrie, C.A., 2014. Abrupt weakening of the summer monsoon in northwest India ∼4100 yr ago. Geology 42 (4), 339–342.

Dixit, Y., Hodell, D.A., Giesche, A., Tandon, S.K., Gazquez, F., Saini, H.S., Skinner, L.C., Mujtaba, S.A.I., Pawar, V., Singh, R.N., Petrie, C.A., 2018. Intensified summer monsoon and the urbanization of Indus Civilization in northwest India. Sci. Rep. https://doi.org/10.1038/s41598-018-22504-5.

Drysdale, R., Zanchetta, G., Hellstrom, J., Maas, R., Fallick, A., Pickett, M., Cartwright, I., Piccini, L., 2006. Late Holocene drought responsible for the collapse of Old World civilizations is recorded in an Italian cave flowstone. Geology 34, 101–104.

Dykoski, C.A., Edwards, R.L., Cheng, H., et al., 2005. A high-resolution, absolute- dated Holocene and deglacial Asian monsoon record from Dongge Cave, China. Earth Planet Sci. Lett. 233, 71–86.

Dutta, S., Gupta, A.K., Wünnemann, B., Yan, D., 2018. A long arid interlude in the Indian summer monsoon during ∼4,350 to 3, 450 cal. yr BP contemporaneous to displacement of the Indus valley civilization. Quat. Int. https://doi.org/10.1016/j.quaint.2018.04.005.

Enzel, Y., Ely, L.L., Mishra, S., Ramesh, R., Amit, R., Lazar, B., Rajaguru, S.N., Baker, V.R., Sandler, A., 1999. High – resolution Holocene environmental changes in the Thar Desert, north western India. Science 284, 125–128.

Enzel, Y., Bookman, R., Sharon, D., Gvirtzman, H., Dayan, U., Ziv, B., Stein, M., 2003. Late Holocene climates of the Near East deduced from Dead Sea level variations and modem regional winter rainfall. Quat. Res. 60 (3), 263–273.

Erdtman, G., 1943. An Introduction to Pollen Analysis. Chronica Botanica Company, Waltham, MA.

Faure, G., 1977. Principles of Isotope Geology. John Wiley & Sons, New York.

Faure, G., Mensing, T.M., 2004. Isotope: Principles and Applications. John Wiley & Sons, New York.

Feng, Z.-D., Tang, L.Y., Wang, H.B., et al., 2006. Holocene vegetation variations and the associated environmental changes in the western part of the Chinese Loess Plateau. Paleogeogr. Paleoclimatol. Paleoecol. 241, 440–456.

Feng, Z.-D., An, C.B., Tang, L.Y., et al., 2004. Stratigraphic evidence of a megahu- mid climate between 10,000 and 4000 years B.P. in the western part of the Chinese Loess Plateau. Global Planet. Change 43, 145–155.

Frumkin, A., Kadan, G., Enzel, Y., Eyal, Y., 2001. Radiocarbon chronology of the Holocene Dead Sea: attempting a regional correlation. Radiocarbon 43 (3), 1179–1190.

Gao, H., Zhu, C., Xu, W., 2007. Environmental change and cultural response around 4200 cal. yr BP in the Yishu River Basin, Shandong. J. Geogr. Sci. 63, 285–292 (in Chinese with English Abstract).

Gasse, F., Fontes, J.C., Van Campo, E., Wei, K., 1996. Holocene environmental changes in lake Bangong basin (western Tibet). Part 4: discussion and conclusion. Palaeogeogr. Palaeoclimatol. Palaeoecol. 120, 79–92.

Gasse, F., Van Campo, E., 1994. Abrupt post-glacial climate events in West Asia and North Africa monsoon domains. Earth Planet Sci. Lett. 126 (4), 435–456.

Guiot, J., Goeury, C., 1996. PPPBase, a software for statistical analysis of paleoecological and paleoclimatological data. Dendrochronologia 14, 295–300.

Giosan, L., et al., 2012. Fluvial landscapes of the Harappan civilization. Nat. Acad. Sci. Proc. 109, E1688–E1694.

Grimm, E.C., 1987. CONISS: a FORTRAN 77 program for stratigraphically constrained cluster analysis by the method of incremental sum of squares. Comput. Geosci. 13, 13–35.

Grimm, E.C., 2004. TILIA and TG View 2.0.2. Illinois State Museum, Springfield IL.

Gupta, A.K., Anderson, D.M., Overpeck, J.T., 2003. Abrupt changes in the asian southwest monsoon during the Holocene and their links to the north atlantic ocean. Nature 421, 354–357.

Herzschuh, U., Winter, K., Wünnemann, B., Li, S., 2006. A general cooling trend on the central Tibetan Plateau throughout the Holocene recorded by the Lake Zigetang pollen spectra. Quat. Int. 154 (155), 113–121.

Hong, Y.T., Hong, B., Lin, Q.H., et al., 2005. Inverse phase oscillations between the East Asian and Indian Ocean summer monsoons during the last 12000 years and paleo-El Nino. Earth Planet Sci. Lett. 231, 337–346.

Hong, Y.T., Hong, B., Lin, Q.H., 2003. Correlation between Indian Ocean summer monsoon and North Atlantic climate during the Holocene. Earth Planet Sci. Lett. 211 (3–4), 371–380.

Hong, Y.T., Wang, Z., Jiang, H., et al., 2001. A 6000-year record of changes in drought and precipitation in northeastern China based on a δ13C time series from peat cellulose. Earth Planet Sci. Lett. 185, 111–119.

Hu, C.Y., Henderson, G.M., Huang, J.H., et al., 2008. Quantification of Holocene Asian monsoon rainfall from spatially separated cave records. Earth Planet Sci. Lett. 266, 221–232.

Jian, Z.M., Wang, P.X., Saito, Y., Wang, J., Pflaumann, U., Oba, T., Cheng, X., 2000. Holocene variability of the Kuroshio Current in the Okinawa trough, northwestern pacific ocean. Earth Planet Sci. Lett. 184, 305–319.

Jiang, W., Leroy, S.A.G., Ogle, N., Chu, G., Wang, L., Liu, J., 2008. Natural and anthropogenic forest fires recorded in the Holocene pollen record from a Jinchuan peat bog, northeastern China. Palaeogeogr. Palaeoclimatol. Palaeoecol. 261 (1–2), 47–57.

Jiang, W., Guo, Z., Sun, X., Wu, H., Chu, G., Yuan, B., Hatte, C., Guiot, J., 2006. Reconstruction of climate and vegetation changes of lake Bayanchagan (Inner Mongolia): Holocene variability of the east asian monsoon. Quat. Res. 65, 411–420.

Jin, G.Y., Liu, T.S., 2002. Mid-Holocene climate change in North China, and the effect on cultural development. Chin. Sci. Bull. 47, 408–413.

Juggins, S., 2016. Rioja: analysis of quaternary Science data, R package version (0.9-7). http://cran.r–project.org/package = rioja.

Kaniewski, D., Paulissen, E., Van Campo, E., Al-Maqdissi, M., Bretschneider, J., Van Lerberghe, K., 2008. Middle East coastal ecosystem response to middle-to-late Holocene abrupt climate changes. Proc. Natl. Acad. Sci. Unit. States Am. 105 (37), 13941–13946.

Kato, M., Fukusawa, H., Yasuda, Y., 2003. Varved lacustrine sediments of lake Tougou Cike, western Japan, with reference to Holocene sea-level changes in Japan. Quat. Int. 105 (1), 33–37.

Kesari, G.K., 2010. Geology and Mineral Resources of Arunachal Pradesh. Geological Survey of India, Arunachal Pradesh, vol. 30 Geological Survey of India, Miscellaneous Publication (IV) (I) (i).

Kotlia, B.S., Sanwal, J., Phartiyal, B., Joshi, L.M., Trivedi, A., Sharma, C., 2010. Late Quaternary climatic changes in the eastern Kumaun Himalaya, India, as deduced from multi-proxy studies. Quat. Int. 213, 44–45.

Kotlia, B.S., Singh, A.K., Joshi, L.M., Dhaila, B.S., 2015. Precipitation variability in the indian central Himalaya during last ca. 4,000 years inferred from a speleothem record: impact of indian summer monsoon (ISM) and westerlies. Quat. Int. 371, 244–353.

Kramer, A., Herzschuh, U., Mischke, S., Zhang, C., 2010. Holocene treeline shifts and monsoon variability in the Hengduan Mountains (southeastern Tibetan Plateau), implications from palynological investigations. Palaeogeogr. Palaeoclimatol. Palaeoecol. 286, 23–41.

Krishnan, R., Kumar, V., Sugi, M., Yoshimura, J., 2009. Internal feedbacks from monsoon-midlatitude interactions during droughts in the Indian summer monsoon. J. Atmos. Sci. 66 (3), 553–578.

Laskar, A.H., 2011. Stable and Radioactive Carbon in Indian Soils: Implications to Soil Carbon Dynamics. Ph.D. Thesis, Mohanlal Sukhadia University, Udaipur, India.

Laskar, A.H., Yadava, M.G., Ramesh, R., 2012. Radiocarbon and stable carbon isotopes in two soil profiles from northeast India. Radiocarbon 54 (1), 81–89.

Lemcke, G., Sturm, M., 1997. δ18O and trace element measurements as proxy for the reconstruction of climate changes at Lake Van (Turkey): preliminary results. In: Dalfes, N., Kukla, G., Weiss, H. (Eds.), Third Millennium BC Climate Change and Old World Collapse. Springer, Berlin, pp. 653–678.

Liu, F., Feng, Z., 2012. A dramatic climatic transition at 4000 cal. yr BP and its cultural responses in Chinese cultural domains. Holocene 22, 1181–1197.

Liu, K., Yao, Z., Thompson, L.G., 1998. A pollen record of Holocene climatic changes from the Dunde ice cap, Qinghai-Tibetan Plateau. Geology 26, 135–138.

Liu, X.Q., Shen, J., Wang, S.M., 2002. Pollen assemblages and climatic changes in the Qinghai Lake during the past 16 ka. Chin. Sci. Bull. 47 (17), 1351–1355 (in Chinese with English Abstract).

MacDonald, G., 2011. Potential influence of the pacific ocean on the indian summer monsoon and Harappan decline. Quat. Int. 299, 140–148.

Marchant, R., Hooghiemstra, H., 2004. Rapid environmental change in African and South American tropics around 4000 years before present: a review. Earth Sci. Rev. 66, 217–260.

Marshall, S.J., 1931. Mohenjo-daro and the Indus Civilization 3 Vols Arthur Probsthain, London.

Michaelsen, J., 1987. Cross–validation in statistical climate forecast models. J. Appl. Meteorol. Climatol. 26, 1589–1600.

Migowski, C., Stein, M., Prasad, S., Negendank, J.F., Agnon, A., 2006. Holocene climate variability and cultural evolution in the Near East from the Dead Sea sedimentary record. Quat. Res. 66 (3), 421–431.

Mischke, S., Zhang, C., 2010. Holocene cold events on the Tibetan Plateau. Global Planet. Change 72 (3), 155–163.

Mischke, S., Kramer, M., Zhang, C., Shang, H., Herzschuh, U., Erzinger, J., 2008. Reduced early Holocene moisture availability in the Bayan Har Mountains, northeastern Tibetan Plateau, inferred from a multi-proxy lake record. Palaeogeogr. Palaeoclimatol. Palaeoecol. 267, 59–76.

Mischke, S., Rajabov, I., Mustaeva, N., Zhang, C., Herzschuh, U., Boomer, I., Brown, E.T., Andersen, N., Myrbo, A., Ito, E., Schudack, M.E., 2010a. Modern hydrology and late Holocene history of Lake Karakul, eastern Pamirs (Tajikistan): a reconnaissance study. Palaeogeogr. Palaeoclimatol. Palaeoecol. 289, 10–24.

Mischke, S., Zhang, C., Börner, A., Herzschuh, U., 2010b. Lateglacial and Holocene variation in aeolian sediment flux over the northeastern Tibetan Plateau recorded by laminated sediments of a saline meromictic lake. J. Quat. Sci. 25, 162–177.

Morrill, C., Overpeck, J.T., Cole, J.E., Liu, K., Shen, C., Tang, L., 2006. Holocene variations in the Asian monsoon inferred from the geochemistry of lake sediments in central Tibet. Quat. Res. 65, 232–243.

Mügler, I., Gleixner, G., Günther, F., Mäusbacher, R., Daut, G., Schütt, B., Berking, J., Schwalb, A., Schwark, L., Xu, B., Yao, T., Zhu, L., Yi, C., 2010. A multi-proxy approach to reconstruct hydrological changes and Holocene climate development of Nam Co, Central Tibet. J. Paleolimnol. 43 (4), 625–648.

Murata, F., Hayashi, T., Matsumoto, J., Asada, H., 2007. Rainfall on the Meghalaya plateau in northeastern India: one of the rainiest places in the world. Nat. Hazards: J. Int. Soc. Prev. Mitig. Nat. Hazards 42 (2), 391–399.

New, M., Lister, D., Hulme, M., Makin, I., 2002. A high–resolution data set of surface climate over global land areas. Clim. Res. 21, 1–25.

Nakamura, A., Yokoyama, Y., Maemoku, H., Yagi, H., Okamura, M., Matsuoka, H., Miyake, N., Osada, T., Adhikari, D.P., Dangol, V., Ikehara, M., Miyairi, Y., Matsuzaki, H., 2016. Weak monsoon event at 4.2 ka recorded in sediment from Lake Rara, Himalayas. Quat. Int. 397, 349–359.

Norbu, L., 2015. A Geographical Analysis of Transhumance Among the Monpa Tribe of Arunachal Pradesh. Rajiv Gandhi University, Itanagar, Arunachal Pradesh, India Ph.D. Thesis.

Parker, A., Eckersley, L., Smith, M.M., Goudie, A., Stokes, S., Ward, S., White, K., Hodson, M., 2004. Holocene vegetation dynamics in the northeastern Rub' al-Khali desert, Arabian Peninsula: a phytolith, pollen and carbon isotope study. J. Quat. Sci. 19 (7), 665–676.

Parker, A., Goudie, A., Stokes, S., White, K., Hodson, M., Manning, M., Kennet, D., 2006. A record of Holocene climate change from lake geochemical analyses in southeastern Arabia. Quat. Res. 66 (3), 465–476.

Peng, Y., Xiao, J., Nakamura, T., Liu, B., Inouchi, Y., 2005. Holocene East Asian monsoonal precipitation pattern revealed by grain-size distribution of core sediments of Daihai Lake in Inner Mongolia of north-central China. Earth Planet Sci. Lett. 233 (3C4), 467–479.

Phadtare, N.R., 2000. Sharp decrease in summer monsoon strength 4000–3500 cal yr B. P. in the Central Higher Himalaya of India based on pollen evidence from alpine peat. Quat. Res. 53, 122–129.

Pokharia, A.K., Agnihotri, R., Sharma, S., Bajpai, S., Nath, J., Kumaran, R.N., Negi, B.C., 2017. Altered cropping pattern and cultural continuation with declined prosperity following abrupt and extreme arid event at ~4,200 yrs BP: evidence from an Indus archaeological site Khirsara, Gujarat, western India. PLoS One 12 (10), e0185684.

Possehl, G., 1997. Climate and the eclipse of the ancient cities of the Indus. In: In: Dalfes, H.N., Kukla, G., Weiss, H. (Eds.), Third Millenium BC Climate Change and Old World Collapse, vol. 1. NATO ASI Springer, New York, pp. 193–244 (49).

Possehl, G.L., 2002. Indus Civilization: a Contemporary Perspective. Altamira Press, Lanham MD.

Postgate, J.N., 1992. Early Mesopotamia. Routledge, New York.

Prasad, S., Enzel, Y., 2006. Holocene paleoclimates of India. Quat. Res. 66 (3), 442–453.

R Core Team, 2016. R: a Language and Environment for Statistical Computing.

Redman, C.L., Crumley, R.C.L., Hassan, F.A., Hole, F., Morais, J., Riedel, F., Scarborough, V.L., Tainter, J.A., Turchin, P., Yasuda, Y., 2007. Group report: millennial perspectives on the dynamic Interaction of climate, people, and resources. In: Costanza, R., Graumlich, L.J., Steffen, W. (Eds.), "Report of the 96th Dahlem Workshop on Integrated History and Future of People on Earth (IHOPE) Berlin, June 12–17, 2005", Sustainability or Collapse? an Integrated History and Future of People on Earth. The MIT Press Cambridge, Massachusetts, pp. 115–150.

Reimer, P.J., et al., 2013. IntCal13 and Marine13 radiocarbon age calibration curves 0–50,000 years cal BP. Radiocarbon 55 (2), 1869–1887.

Roland, T.P., 2012. Was There a '4.2 Kyr Event' in Great Britain and Ireland? Evidence from the Peatland Record. University of Exeter, PhD Thesis.

Roland, T.P., Caseldine, C.J., Charman, D.J., Turney, C.S.M., Amesbury, M.J., 2014. Was there a '4.2 ka event' in Great Britain and Ireland? Evidence from the peatland record. Quat. Sci. Rev. 83, 11–27.

Sarkar, A., Mukherjee, A.D., Bera, M.K., Das, B., Juyal, N., Morthekai, P., Deshpande, R.D., Shinde, V.S., Rao, L.S., 2016. Oxygen isotope in archaeological bioapatites from India: implications to climate change and decline of Bronze Age Harappan civilization. Sci. Rep. 6, 26555.

Schlütz, F., Lehmkuhl, F., 2009. Holocene climatic change and the nomadic Anthropocene in Eastern Tibet: palynological and geomorphological results from the Nianbaoyeze Mountains. Quat. Sci. Rev. 28, 1449–1471.

Schwanghart, W., Schuett, B., Walther, M., 2008. Holocene climate evolution of the Ugii Nuur basin, Mongolia. Adv. Atmos. Sci. 25 (6), 986–998.

Seong, Y.B., Owen, L.A., Yi, C., Finkel, R.C., 2009. Quaternary glaciation of Muztag Ata and Kongur Shan: evidence for glacier response to rapid climate changes throughout the late glacial and Holocene in westernmost Tibet. Geol. Soc. Am. Bull. 121, 348–365.

Shao, X.H., Wang, Y.J., Cheng, H., et al., 2006. Stalagmite record of monsoon climate changes and arid events from Shennongjia of Hubei Province. Chin. Sci. Bull. 51 (1), 80–86 (in Chinese).

Shen, J., Liu, X., Wang, S., Ryo, M., 2005. Palaeoclimatic changes in the Qinghai Lake area during the last 18, 000 years. Quat. Int. 136, 131–140.

Shi, Y., Kong, Z., 1992. Climate and Environment in China. Ocean Press, Beijing (in Chinese).

Shi, Y.F., Kong, Z.C., Wang, S.M., et al., 1993. Mid-Holocene climates and environments in China. Global Planet. Change 7, 219–233.

Singh, G., 1971. The Indus Valley Culture seen in the context of Post –glacial climatic and ecological studies in northwest India. Archaeol. Phys. Anthropol. Ocean. 6 (2), 177–189.

Singh, G., Joshi, R.D., Singh, A.B., 1972. Stratigraphic and radiocarbon evidence for the age and development of three salt lake deposits in Rajasthan, India. Quat. Res. 2 (4), 496–505.

Singh, G., Wasson, J.R., Agrawal, D.P., 1990. Vegetational and seasonal climatic changes since the last full glacial in the Thar Desert, northwestern India. Rev. Palaeobot. Palynol. 64, 351–358.

Singh, R.K., Singh, A., Garnett, S.T., Zander, K.K., Lobsang Tsering, D., 2015. Paisang (*Quercus griffithii*): a keystone tree species in Sustainable agroecosystem management and livelihoods in Arunachal Pradesh, India. Environ. Manag. 55, 187–204.

Stanley, J., Krom, M., Cliff, R.A., Woodward, J.C., 2003. Nile flow failure at the end of the Old Kingdom, Egypt: Strontium isotopic and petrologic evidence. Geoarchaeology 18, 395–402.

Staubwasser, M., Sirocko, F., Grootes, P.M., Segl, M., 2003. Climate change at the 4.2 ka BP termination of the Indus valley civilization and Holocene south Asian monsoon variability. Geophys. Res. Lett. 30 1425–1425.

Tao, J., Chen, M.T., Xu, S.Y., 2006. A Holocene environmental record from the southern Yangtze River delta, eastern China. Palaeogeogr. Palaeoclimatol. Palaeoecol. 230, 204–229.

Tarasov, P., Jin, G.Y., Wagner, M., 2006. Mid-Holocene environmental and human dynamics in Northeastern China reconstructed from pollen and archaeological data. Palaeogeogr. Palaeoclimatol. Palaeoecol. 241, 284–300.

ter Braak, C.J.F., Juggins, S., 1993. Weighted averaging partial least squares regression (WA–PLS): an improved method for reconstruction environmental variables from species assemblages. Hydrobiologia 269, 485–502.

ter Braak, C.J.F., Šmilauer, P., 2012. CANOCO Reference Manual and User's Guide: Software for Ordination, Version 5.0. Microcomputer Power, Ithaca, USA, pp. 496.

Thompson, L., Mosley –Thompson, E., Davis, M., Henderson, K., Brecher, H., Zagorodnov, V., Mashiotta, T., Lin, P., Mikhalenko, V., Hardy, D., 2002. Kilimanjaro ice core records, evidence of Holocene climate change in tropical Africa. Science 298, 589–593.

Thompson, L.G., Yao, T., Davis, M.E., Henderson, K.A., Mosley-Thompson, E., Lin, P.-N., Beer, J., Synal, H.-A., Cole-Dai, J., Bolzan, J.F., 1997. Tropical climate instability: the last glacial cycle from a Qinghai–Tibetan Ice Core. Science 276, 1821–1825.

Thompson, R., Oldfield, F., 1986. Environmental Magnetism. Allen and Unwin Press, London, pp. 220.

Trivedi, A., Chauhan, M.S., 2009. Holocene vegetation and climate fluctuations in northwest Himalaya, based on pollen evidence from Surinsar Lake, Jammu region, India. J. Geol. Soc. India 74, 402–412.
Walter, H., Lieth, H., 1967. Klimadiagram – Weltatlas. VEB Gautav Fischer Verlage, Jena.
Wang, F., Fan, C.Y., 1987. Climatic changes in the Qinghai-Xizang (Tibetan) region of China during the Holocene. Quat. Res. 28, 50–60.
Wang, S., Wang, F., 1992. Lacustrine records of the mid-Holocene megath- ermal climate in China. In: Shi, Y.F., Kong, Z.C. (Eds.), Holocene Mega- Thermal Climates and Environments in China. Ocean Press, Beijing, pp. 146–152 (in Chinese).
Wang, S.Y., Lu, H.Y., Liu, J.L., et al., 2007. Pollen-recorded early Holocene climatic optimum from Huguangyan Maar sediments. Chin. Sci. Bull. 52 (11), 1285–1291 (in Chinese).
Wang, Y., Cheng, H., Edwards, R., et al., 2005. The Holocene asian monsoon: links to solar changes and North Atlantic climate. Science 308, 854–857.
Wei, K., Gasse, F., 1999. Oxygen isotopes in lacustrine carbonates of West China revisited: implications for post glacial changes in summer monsoon circulation. Quat. Sci. Rev. 18 (12), 1315–1334.
Weiss, H., 2000. Beyond the Younger dryas—collapse as adaptation to abrupt climatic change in ancient west Asia and the eastern mediterranean. In: Bawden, G., Reycraft, R. (Eds.), Confronting Natural Disaster, Engaging the Past to Understand the Future. University of New Mexico Press, Albuquerque, pp. 75–98.
Weiss, H., Bradley, R.S., 2001. What Drives societal collapse? Science 291, 609–610.
Weiss, H., Courty, M., Wetterstrom, W., Guichard, F., Senior, L., Meadow, R., Curnow, A., 1993. The genesis and collapse of third millennium north Mesopotamian civilization. Science 261, 995–1004.
Wen, R.L., Xiao, J.L., Chang, Z.G., et al., 2010a. Holocene precipitation and temperature variations in the East Asian monsoonal margin from pollen data from Hulun Lake in northeastern Inner Mongolia, China. Boreas 39 (2), 262–272.
Wen, R.L., Xiao, J.L., Chang, Z.G., et al., 2010b. Holocene climate changes in the mid--high-latitude-monsoon margin reflected by the pollen record from Hulun Lake, northeastern Inner Mongolia. Quat. Res. 73 (2), 293–303.
Wilkinson, T.G., 1997. Holocene environments of the high plateau, Yemen: recent geoarchaeological investigations. Geoarchaeology 12 (8), 833–864.
Wu, Y., Lücke, A., Jin, Z., Wang, S., Schleser, G.H., Battarbee, R.W., Xia, W., 2006. Holocene climate development on the central Tibetan Plateau: a sedimentary record from Cuoe Lake. Palaeogeogr. Palaeoclimatol. Palaeoecol. 234, 328–340.
Yang, T.-N., Lee, T.-Q., Meyers, P.A., Song, S.-R., Kao, S.-J., Löwemark, L., Chen, R.-F., Chen, H.-F., Wei, K.-Y., Fan, C.-W., Shiau, L.-J., Chiang, H.-W., Chen, Y.-G., Chen, M.T., 2011. Variations in monsoonal rainfall over the last 21kyr inferred from sedimentary organic matter in Tung-Yuan Pond, southern Taiwan. Quat. Sci. Rev. 30 (23–24), 3413–3422.
Yao, T., Thompson, L.G., 1992. Trends and features of climatic changes in the past Tibet. Quat. Int. 45 (46), 123–134.
Yu, X., Zhou, W., Franzen, L.G., Xian, F., Cheng, P., Jull, A.J.T., 2006. High resolution peat records for Holocene monsoon history in the eastern Tibetan Plateau. Science in China (Series D) 49, 615–621.
Zhang, L.S., Fang, X.Q., Ren, G.Y., et al., 1997. Holocene environmental changes along the border between agricultural and nomadic cultures in northern China. Earth Sci. Front. 4 (12), 127–136 (in Chinese with English Abstract).
Zhang, M.L., Yuan, D.X., Lin, Y.S., et al., 2004. A 6000-year high-resolution climatic record from a stalagmite in Xiangshui Cave, Guilin, China. Holocene 14 (5), 697–702.
Zheng, Z., Wang, J.H., Wang, B., 2003. High-resolution climate reconstruction from Huguangyan maar sediments, Hainan province of China. Chin. Sci. Bull. 48 (3), 282–286 (in Chinese with English Abstract).
Zhu, C., Zhong, Y.S., Zheng, C.G., et al., 2007. Relationship of archaeological sites distribution and environmental changes from the paleolithic age to the warring States times in Hubei province. Acta Geograph. Sin. 62 (3), 227–242 (in Chinese with English Abstract).
Zhu, L., Wu, Y., Wang, J., Lin, X., Ju, J., Xie, M., Li, M., Mäusbacher, R., Schwalb, A., Daut, G., 2009b. Environmental changes since 8.4ka reflected in the lacustrine core sediments from Nam Co, central Tibetan Plateau, China. Holocene 18, 831–839.
Zhu, L., Zhen, X., Wang, J., Lü, H., Xie, M., Kitagawa, H., Possnert, G., 2009a. A 30, 000-year record of environmental changes inferred from Lake Chen Co, Southern Tibet. J. Paleolimnol. 42, 343–358.